Master Thesis

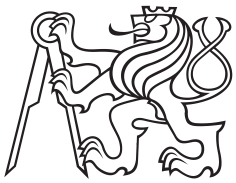

Czech Technical University in Prague

F3

Faculty of Electrical Engineering
Department of Circuit Theory

Functional reorganization of brain networks after stroke

Bc. Vojtěch Kumpošt

Supervisor: prof. MUDr. Přemysl Jiruška, Ph.D.
Field of study: Biomedical Engineering and Informatics
Subfield: Biomedical Engineering
May 2019

MASTER'S THESIS ASSIGNMENT

I. Personal and study details

Student's name: **Kumpošt Vojtěch** Personal ID number: **420401**

Faculty / Institute: **Faculty of Electrical Engineering**

Department / Institute: **Department of Circuit Theory**

Study program: **Biomedical Engineering and Informatics**

Branch of study: **Biomedical Engineering**

II. Master's thesis details

Master's thesis title in English:

Functional Reorganization of Brain Networks after Stroke

Master's thesis title in Czech:

Funkční reorganizace mozkových sítí po cévní mozkové příhodě

Guidelines:

1. Estimate functional connectivity from hdEEG recordings obtained from patients after stroke.
2. Create a database of neuropsychological tests and parameterize individual tests.
3. Determine global and local parameters of the networks.
4. Correlate cognitive performance and network parameters.

Bibliography / sources:

[1] Ed Bullmore, Olaf Sporns. Complex brain networks: graph theoretical analysis of structural and functional systems. Nature Reviews Neuroscience, 10: 186-198, 2009.
[2] Mikail Rubinov, Olaf Sporns. Complex network measures of brain connectivity: uses and interpretations. NeuroImage, 52: 1059–1069, 2010.
[3] Cornelis J. Stam. Modern network science of neurological disorders. Nature Reviews Neuroscience, 15: 683-695, 2014
[4] Olaf Sporns. Networks of the Brain. The MIT Press, 2010.
[5] Martin Vinck, Robert Oostenveld, Marijn van Wingerden, Franscesco Battaglia, Cyriel M.A. Pennartz. An improved index of phase-synchronization for electrophysiological data in the presence of volume-conduction, noise and sample-size bias. NeuroImage, 55: 1548–1565, 2011.

Name and workplace of master's thesis supervisor:

prof. MUDr. Přemysl Jiruška, Ph.D., Institute of Physiology CAS, Prague

Name and workplace of second master's thesis supervisor or consultant:

Ing. Radek Janča, Ph.D., Department of Circuit Theory, FEE

Date of master's thesis assignment: **12.12.2018** Deadline for master's thesis submission: **24.05.2019**

Assignment valid until: **30.09.2020**

prof. MUDr. Přemysl Jiruška, Ph.D. Supervisor's signature	doc. Ing. Radoslav Bortel, Ph.D. Head of department's signature	prof. Ing. Pavel Ripka, CSc. Dean's signature

III. Assignment receipt

The student acknowledges that the master's thesis is an individual work. The student must produce his thesis without the assistance of others, with the exception of provided consultations. Within the master's thesis, the author must state the names of consultants and include a list of references.

Date of assignment receipt	Student's signature

Acknowledgements

I sincerely thank Mgr. Veronika Matušková for the help with the interpretation and parametrisation of the neuropsychological tests.

I would also like to express my gratitude to prof. MUDr. Přemysl Jiruška, Ph.D. for his guidance, feedback and mainly the opportunity to work on this exciting topic.

Declaration

I declare that the presented work was developed independently and that I have listed all sources of information used within it in accordance with the methodical instructions for observing the ethical principles in the preparation of university theses.

Prague, May 22, 2019

Abstract

The brain is a complex system that can be described as a network consisting of nodes (brain regions) and links (connections). This network undergoes functional reorganisations after a stroke and in cognitive decline. Therefore, we assume that the post-stroke cognitive deficit is related to the disruption of the brain network caused by the stroke. This thesis aims to find possible relationships between the network and cognitive parameters in post-stroke patients. I evaluated the resting-state closed-eye electroencephalographic (EEG) data and the neuropsychological tests for 45 post-stroke patients. An automatic modular pipeline was developed to process the EEG recordings and estimate network parameters. The algorithm includes removal of the cardiac and ocular artefacts based on the independent component analysis. The functional connectivity was estimated based on coherence, imaginary coherence and the weighted phase lag index in three frequency bands, theta, alpha and beta. In cooperation with a neuropsychologist, we proposed a parametrisation of the neuropsychological tests and converted them into cognitive parameters. Finally, I used the Kendall rank correlation coefficient to correlate the network and cognitive parameters. The thesis showed some interesting trends in the theta and beta bands for imaginary coherence. However, statistical evidence for those trends was rather weak when I accounted for the repeated testing. Consequently, I cannot state there is a relationship between the cognitive and network parameters in post-stroke patients.

Keywords: brain, stroke, electroencephalography, brain networks, graph theory

Supervisor: prof. MUDr. Přemysl Jiruška, Ph.D.
Oddělení vývojové epileptologie,
Fyziologický ústav AV ČR,
Vídeňská 1083,
14220 Praha 4

Abstrakt

Mozek je komplexní systém, který je možné popsat jako síť s vrcholy (oblastmi mozku) a hranami (spojeními). Tato mozková síť je narušena po cévní mozkové příhodě a při zhoršování kognitivních funkcí. Z tohoto důvodu předpokládáme, že kognitivní deficit po cévní mozkové příhodě je následkem narušení mozkové sítě. Cílem této práce je vyhodnotit vztah mezi síťovými a kognitivními parametry u pacientů po cévní mozkové příhodě. Vyhodnotil jsem klidovou elektroencefalografickou (EEG) aktivitu a neuropsychologické testy pro 45 pacientů po cévní mozkové příhodě. Vytvořil jsem automatizovaný modulární algoritmus na zpracování EEG a odhad síťových parametrů. Tento algoritmus zahrnuje odstranění srdečních a očních artefaktů pomocí analýzy hlavních komponent. Funkční konektivita byla odhadnuta na základě koherence, imaginární koherence a váženého indexu fázového zpoždění v théta, alfa a beta frekvenčních pásmech. Ve spolupráci s neuropsycholožkou jsme připravili metodu parametrizace neuropsychologických testů a jejich převod do kognitivních parametrů. Vztah mezi síťovými a kognitivními parametry byl odhadnut pomocí Kendallova koeficientu korelace. Tato práce ukázala zajímavé trendy v théta a beta pásmu pro imaginární koherenci. Nicméně po korekci vícenásobného testování tyto trendy nebyly dostatečné statisticky významné. Proto nemohu konstatovat, že bych pozoroval závislost mezi síťovými a kognitivními parametry u pacientů po cévní mozkové příhodě.

Klíčová slova: mozek, cévní mozková příhoda, electroencefalografie, mozkové sítě, teorie grafů

Překlad názvu: Funkční reorganizace mozkových sítí po cévní mozkové příhodě

Contents

Figures

Tables

Chapter 1

Introduction

Stroke is a common neurological disease that can result in many post-stroke complications, among which one of the most serious is a cognitive deficit. The post-stroke cognitive deficit presents a great burden for the patient and a better understanding of its underlying mechanisms would be beneficial for future improvements in the rehabilitation and recovery of the post-stroke patients. One way to better understand the changes that the brain undergoes after a stroke is to study the alterations in the connections among the distant brain regions.

In this thesis, I aim to shed some light on this problem by studying the reorganisation of the functional brain networks in the patients after a stroke. I will use EEG recordings to estimate network parameters and neuropsychological tests to estimate cognitive parameters. Then, I will compare those two to evaluate if there is any relationship between the network reorganisation and the level of the cognitive decline in post-stroke patients.

1.1 Network construction

Brain networks can be structural or functional. The structural networks describe actual anatomical connections between the brain regions. In human subjects, anatomical connections are usually reconstructed using diffusion tensor imaging (DTI).

On the other hand, functional networks do not represent actual physical connections of the brain regions but rather statistical associations between the recorded signals. Functional connectivity networks are usually constructed using functional magnetic resonance imaging (fMRI), in particular, blood-oxygen-level-dependent imaging (BOLD). In those networks, the nodes are groups of voxels of fMRI and the links between them correspond to the correlations between the BOLD signals.

Functional networks can also be estimated from electroencephalography (EEG) and magnetoencephalography (MEG) signals. In those cases, the nodes are usually equal to the recording sensors, and the links are computed based on the correlations between the time series the sensors generate.

Regardless of the chosen technology, brain networks are constructed following four main steps (Figure 1.1) [1]:

1. Definition of the network nodes (e.g. brain regions, EEG electrodes, MEG sensors, ...).
2. Estimation of the links between the nodes (e.g. correlations, white matter tracts, ...).
3. Assembly of the links into a single graph, which includes thresholding and binarisation of the network.
4. Parametrisation and analysis of the network parameters.

The resulting graphs can be weighted or unweighted and directed or undirected [2]. The directed graphs consist of directed links that specify the direction of the information transfer between the nodes. However, much more common in the literature is to work with the undirected graphs that link the nodes without additional information about causality.

The links in the weighted graphs are associated with a value that represents their strength, meanwhile, in the unweighted (binary) graphs the connection is simply either existing (1) or non-existing (0). The unweighted graphs are usually prefered because they lead to much easier analysis and they still carry enough information about the overall topology of the network.

The construction of the graphs also includes thresholding. During this procedure, the weak links that present spurious connections and hinder the real topology of the graph are removed. The choice of a proper threshold is an arbitrary choice that can affect the analysis to a great extent. Different thresholds will generate graphs of varying density and so the graphs are often explored over a range of several thresholds [1].

Recently, there were proposed some algorithms that do not require a choice of an arbitrary threshold such as the minimum spanning tree, the cluster-span threshold and the union of shortest paths. Even though, those algorithms present an exciting alternative to the usual approach, further research in their correct interpretation and use is still needed [3].

1.2 Network organisation

1.2.1 Network parameters

The brain is a complex network that consists of multiple nodes (brain regions) and links (connections) between them. Each node receives information from other nodes, process it and then forward it through the links to other nodes of the network. In this way, complex brain functions, like cognition and sensation, emerge [4]. It is important to emphasise that those complex functions are not located at one place in the brain, but rather proper coordination of distant brain regions is needed to make them work correctly. The main three concepts that are usually examined in the graph theoretical studies are functional integration (global parameters), functional segregation (local parameters) and centrality (Figure 1.2) [2].

Functional integration is mainly represented by the concept of the minimum path length, which is the minimum number of edges that must be traversed to go from one node to another [1]. The average minimum path length between all the pairwise combinations of the nodes is called the characteristic path length [2].

Functional segregation describes the ability of a network to locally process information in the groups of highly interconnected nodes. The main concept of functional segregation is the clustering coefficient which is the number of connections that exist between the node's neighbours as a proportion of the maximum number of possible connections among them [1].

Centrality identifies important nodes (hubs) that interact with many other nodes and facilitate the majority of the information transfer in the network. The most basic measure of centrality is a degree which is the number of links connected to a specific node. Other measures of centrality are, for example, betweenness centrality and closeness centrality. Betweenness centrality is the fraction of all shortest paths in the network that pass through a given node and closeness centrality is the inverse of the average shortest path length from one node to all other nodes in the network [2].

1.2.2 Networks in health and disease

Healthy brain's networks have a so-called small-world organisation that manifests by high clustering coefficient and short characteristic path length (Figure 1.3). The advantages of this organisation are an excellent global effectivity of the information transfer with minimal wiring cost. That is achieved by a scale-free (power law) distribution of the degrees where most of the nodes are connected to their nearest neighbours within their module, and only few hub nodes facilitate the information transfer on long distances between the communities. Furthermore, those essential hub nodes are densely interconnected into so-called rich clubs.

The brain networks were shown to change under many neurological diseases including dementia, multiple sclerosis, traumatic brain injury and epilepsy. The network organisation under those conditions deviate from the optimal pattern of small-worldness. This deviation is becoming stronger with the extension of the structural damage, the severity of the clinical symptoms and disease duration. One of the most consistent findings in neurological diseases was a failure of the hub nodes [3].

1.2.3 Post-stroke connectivity

Stroke is a common neurological disease that commonly results from ischemia which is arterial occlusion that interrupts the blood supply to cerebral tissue [6]. Even though stroke is a focal insult, it induces changes distant from the affected anatomical region and changes the nature of the whole-brain network (Figure 1.4). Therefore, the whole-brain connectivity might be a better predictor of the behavioural deficits than a mere location of the insult. Multiple fMRI studies found changes of post-stroke connectivity related to

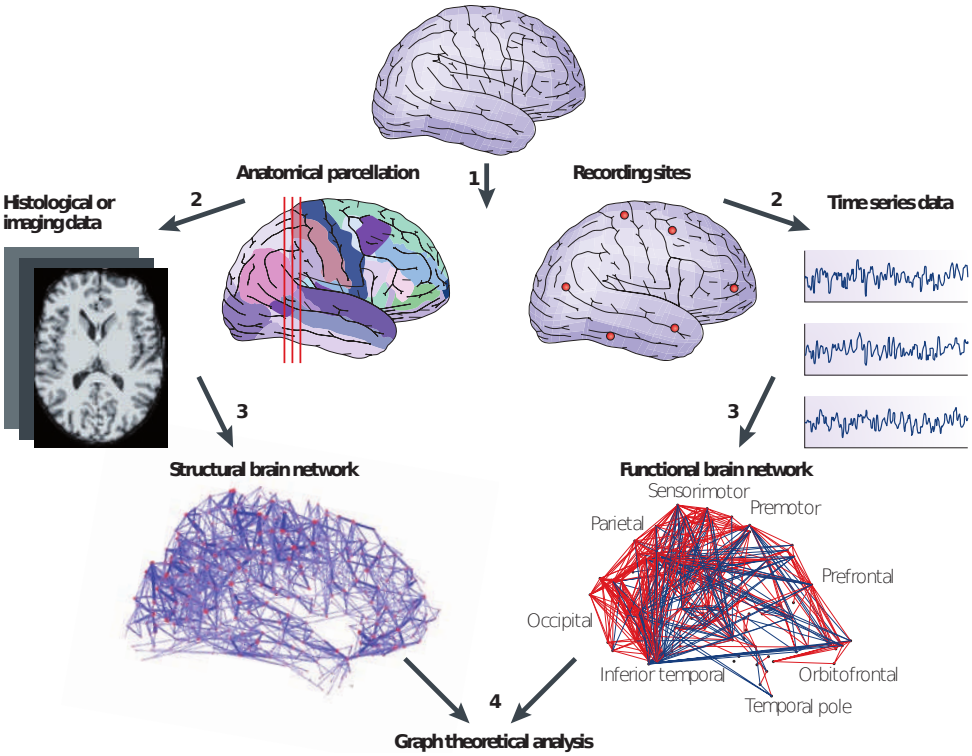

Figure 1.1: Construction of structural and functional brain networks consists of four steps. First, the network nodes are defined. Second, the associations (links) between the nodes are estimated. Third, a graph is constructed by compiling all pairwise associations between the nodes. Four, the graph parameters are calculated and analysed (source: Bullmore and Sporns [1]).

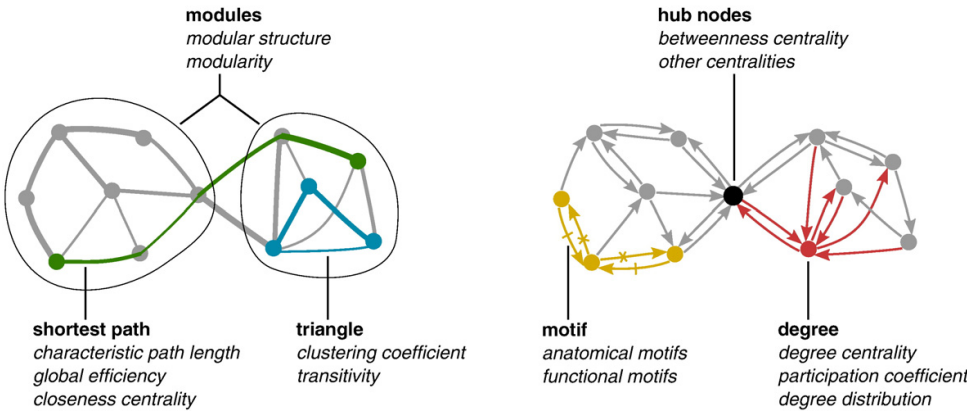

Figure 1.2: The most fundamental concepts are the shortest path, triangle, degree and hubs. The shortest path (in green) is a measure of global efficiency, triangles (in blue) measure local efficiency, and node degrees (in red) measure the importance of the nodes in the network. Hubs (in black) are nodes that facilitate most of the information transfer and are described by the centrality parameters (source: Rubinov and Sporns [2]).

attention, language, motor function and memory [7]. Damage of the hub nodes leads to more severe consequences than the loss of less significant nodes [6]. Interestingly, there were also observed changes in brain connectivity over the time of recovery and as a response to treatment [3].

1.3 EEG functional connectivity

Functional connectivity in human subjects is usually recorded by noninvasive methods such as electroencephalography (EEG), magnetoencephalography (MEG) and functional magnetic resonance imaging (fMRI). The particular interest of this thesis is in the EEG that measures connectivity based on the local changes in neuronal activity. The advantages of EEG are that it has high temporal resolution and that the connectivity can be easily measured in distinct frequency bands. The main disadvantage, in comparison to other techniques such as fMRI, is a low spatial resolution of the recording EEG electrodes [8].

The low spatial resolution is mainly caused by the problem of volume conduction (Figure 1.6). The signals of different origins propagate through the conductive environments of the brain, the cerebrospinal fluid, the skull and the scalp before reaching the scalp electrodes. For this reason, the signals generated by scalp electrodes are not necessarily produced by the brain structures right below them [9].

Except for the volume conduction, the signals are also affected by the choice of recording montage. Montage refers to the selection of the input signal pairs whose difference results in the final EEG signals. The most common montages are the common reference, average reference and bipolar montage. The common reference is when the signal of each electrode is compared to the signal of one selected reference electrode that is common for all the channels. The average reference uses the average signal over all channels and subtracts it from the signal of each electrode. Finally, bipolar montage produces channels as differences of signals of near-by electrodes [10].

1.4 EEG studies

In general, the studies on the functional connectivity follow two paradigms, all-to-all connectivity and seed-based connectivity. All-to-all connectivity refers to the applications of the graph analysis as it was described in the previous sections. Seed-based studies choose one region of interest and then calculate how strong are the connections between this region and the rest of the network (other regions). In the next two subsections, I mention some previous studies on stroke and cognitive decline that utilised the EEG functional connectivity.

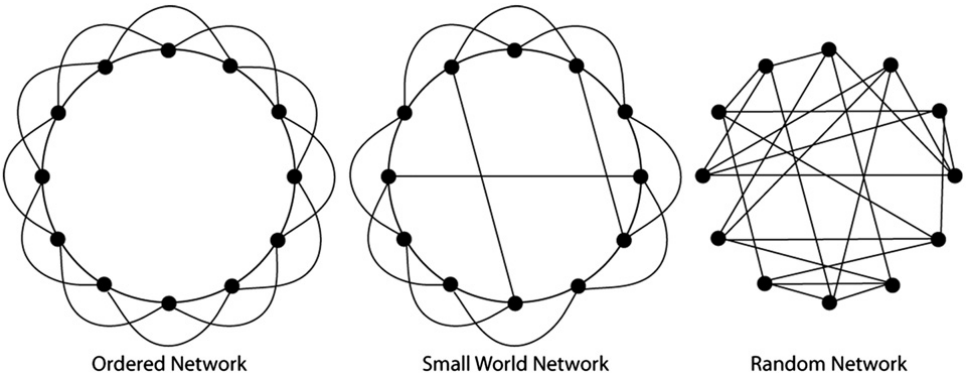

Figure 1.3: A small-world network is an intermediate state between two extremes, an ordered network and a random network. The ordered network has a high clustering coefficient and long characteristic path length, which makes the global information transfer ineffective. The random network is connected by random links and so has a low characteristic path length but limited local information processing. The small-network is an optimal state with high clustering coefficient and few long-distance connections that ensure low characteristic path length (source: van Straaten and Stam [5]).

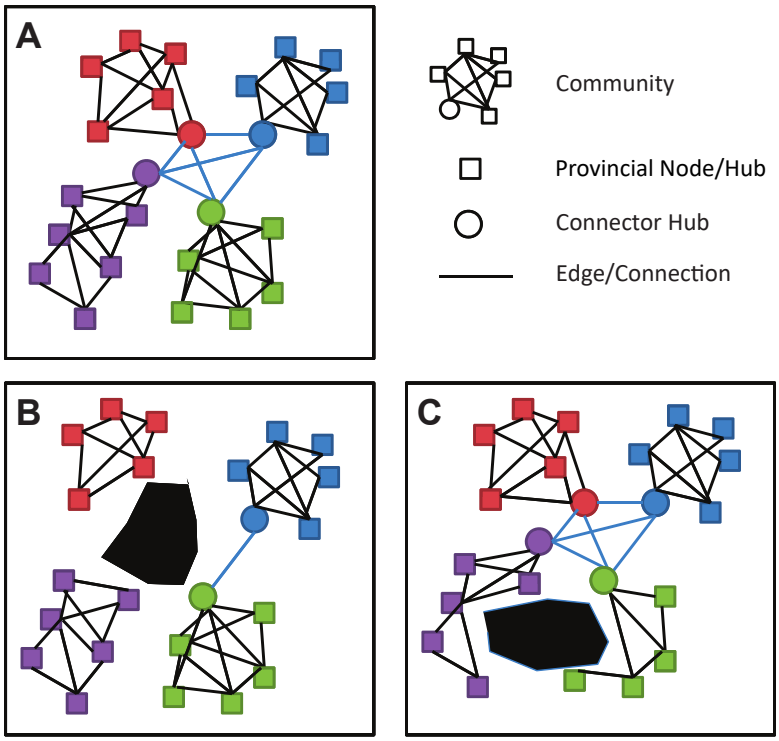

Figure 1.4: Change in integration and segregation of a network after a focal insult. Panel **A** represents a healthy network. In panel **B**, two hub nodes are affected, which lower the global functional integration among the communities. In panel **C**, community members are targeted which results in lower local integration inside of the modules (source: Carrera and Tononi [8]).

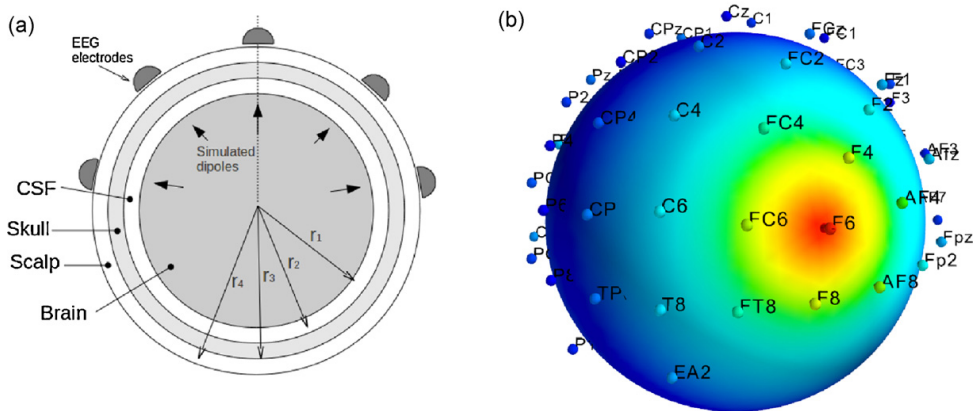

Figure 1.5: In the left, the four sphere head model. The signal generated by the neural structure is diffused by the brain, the cerebrospinal fluid (CSF), the skull and the scalp before reaching the EEG exletrodes. In the right, a simulation of the voltage distribution of a neural source located below the F6 electrode (source: Peraza et al. [9]).

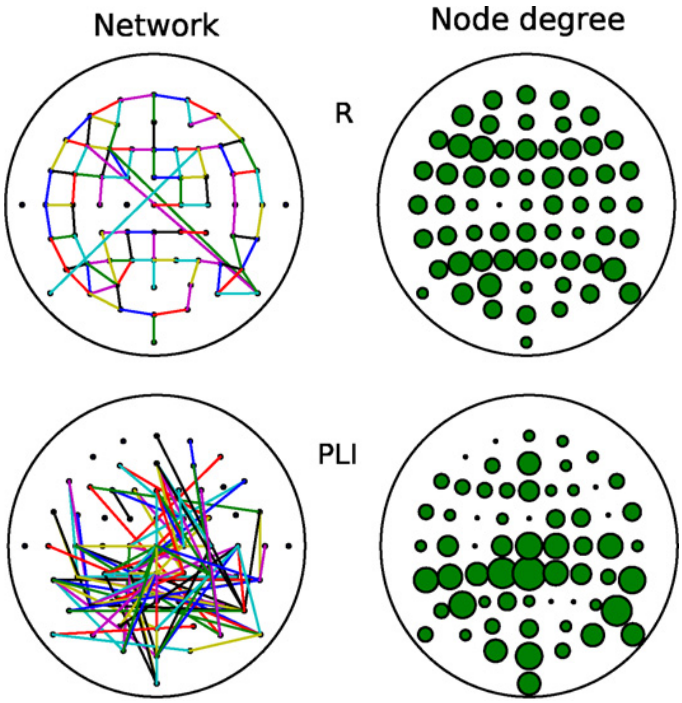

Figure 1.6: Two very common measures of the functional connectivity are coherence (R) and phase lag index (PLI). Coherence is strongly influenced by the volume conduction which causes it looks like a regular matrix. The PLI network has small-world properties and higher variability in the node degree resembling the free-scale topology (source: Peraza et al. [9]).

1.4.1 Stroke

Wu et al. [11] studied the relationship between EEG connectivity and motor deficits across 28 days of intensive therapy. During those 28 days, they recorded four resting-state EEG for 12 post-stroke patients with arm motor deficits. The connectivity was calculated for electrodes covering the ipsilesional primary motor cortex (M1) and ipsilesional frontal-premotor (PM) region. They observed significant correlations between the increased connectivity and motor gains from the therapy.

Wang et al. [12] focused on post-stroke patients with hemianopia. They used the clustering coefficient and characteristic path length to compare the patients with controls but did not find any significant results in the whole-brain connectivity. However, when they focused on local changes, they observed less activity in ipsilesional primary visual cortex and more activity in the ipsilesional temporopolar and orbit frontal areas and the contralesional visual cortex.

Fallani et al. [13] studied functional connectivity in 20 patients during hand motor imagery. They observed that the motor imagery of the affected hand corresponded to significantly lower small-worldness and local efficiency in comparison with the motor imagery of the unaffected hand.

In general, most of the post-stroke functional connectivity studies to this day focus more on motor rather than cognitive deficits. EEG studies are not as common as studies based on fMRI. Frequent observations are decreased connectivity in the affected areas and shift from the small-world to more random networks.

1.4.2 Cognitive decline

Klados et al. [14] recruited 50 seniors with mild cognitive impairment and divided them equally into two groups. One group was control and the other underwent a cognitive and physical training. Resting-state closed-eye EEG connectivity based on coherence was calculated between the time series. Significantly stronger connectivity was found in the beta band (12-30 Hz) for the trained group.

In a similar frequency band (beta, 14-22 Hz), Stam et al. [15] found a decrease in synchronisation likelihood (a type of coherence) in patients with Alzheimer's disease. Furthermore, they observed that the connectivity in this frequency band positively correlated with the results of the Mini-mental state examination.

Vecchio et al. [16] observed a high correlation between small-worldness in the gamma band (30-45 Hz) and memory performance measured by the digit span test.

Recently, Kinney-Lang et al. [17] used imaginary coherence, phase-slope index and weighted phase lag index to correlate connectivity parameters with the level of cognitive impairment in preschool children with epilepsy. They observed significant correlations in medium to high-frequency bands (9-31 Hz) but none on lower frequencies.

Overall, the presented studies found correlations of resting-state EEG connectivity with the cognitive decline on higher frequencies. Those studies are usually based on the resting-state closed-eye networks and the authors often examine multiple frequency bands.

1.5 Aim and objectives

The main aim of this thesis is to evaluate the functional reorganisation of brain networks in patients after a stroke in relationship with the observed cognitive impairments. Four more specific objectives were stated to achieve this goal. The first objective is to construct a signal processing pipeline to estimate functional connectivity from EEG recordings. The second objective is to parametrise the functional connectivity by suitable graph measures. Third, the results of available neuropsychological tests need to be examined and convert into reasonable cognitive parameters. The final objective is to correlate the obtained network and cognitive metrics and evaluate possible relationships between them.

Chapter 2

Methods

2.1 Dataset

2.1.1 Demographics

Patients that showed significant comorbidity with another neurological impairment (Alzheimer's, Parkinson's, bipolar disorder) or clinically significant depression (measured by Geriatric Depression Scale) were excluded from the analysis. Furthermore, the patients that did not finish one or more of the neuropsychological tests were excluded as well. The final sample of subjects that entered the analysis consisted of 45 patients. The mean age of this sample was 63 ± 10 (median 65) years. 16 participants were females and 29 were males, 41 right-handed and 4 left-handed. Each of the 45 participants underwent a neuropsychological examination and an EEG-recording session that were administrated approximately one year after a stroke.

2.1.2 EEG data

The electroencephalographic (EEG) data were recorded on average 376 ± 38 (median 368) days after a stroke and composed of 128 EEG channels and 1 electrocardiographic (ECG) channel. The EEG electrodes were placed according to the 10-5 system (see Figure 2.1) and their signals were referenced to the common average during the recording. Before the analysis, the signals were downsampled to 258 Hz and distributed as MAT-files.

For the examination, the patients were seated in a comfortable chair and a skilful professional guided them through a standardised 20-minute examination sequence (Table 2.1). The standardised sequence included six periods of closed-eye EEG that, in total, resulted in 665 seconds of resting-state EEG signals that were suitable for the estimation of functional connectivity.

2.1.3 Neuropsychological data

The neuropsychological tests were administrated on average 438 ± 87 (median 415) days after a stroke or 62 ± 94 (median 35) days after the EEG examination. The neuropsychological examination battery consisted of a set of tests that

were designed to measure cognitive impairments in patients after a stroke. Their administration usually took around 30 minutes but the actual time might vary depending on the patient's ability to solve the presented tasks. In the rest of this section, I will briefly describe the administrated tests.

Mini-mental state examination

Mini-Mental State Examination (MMSE) is a cognitive screening tool that is extensively used in clinical and research settings to measure cognitive impairments. The test consists of a set of questions that measure performance in various domains ranging from orientation, memory, and attention to the ability to respond to verbal and written commands [18]. This measure was used to evaluate global cognitive performance.

Free and cued selective reminding test

In the Free and cued selective reminding test (FCSRT), a subject is presented with 16 pictures. After the initial presentation, the subject is distracted with solving an unrelated task after which he is asked to recall as many items as possible. Afterwards, the number of successfully recalled items is noted (FR1). Next, the test administrator provides a verbal cue to items that were not freely retrieved and records the number of items additionally recalled after the cue (CR1). This procedure is repeated two more times (FR2, CR2, FR3, CR3). Finally, 30 minutes after the initial presentation, the subject is asked again to recall as many items as possible (delayed free recall, DFR) and a verbal cue is provided for the items he forgot (delayed cued recall, DCR).

Based on the results of this test, four memory measures are calculated

1. Free recall = FR1 + FR2 + FR3
2. Total recall = FR1 + CR1 + FR2 + CR2 + FR3 + CR3
3. Delayed free recall = DFR
4. Delayed total recall = DFR + DCR

Trail making test

The Trail making test consists of two parts, A and B. In part A, the subject is presented with a series of numbers (1, 2, 3, ...) that are randomly located on a sheet of paper. Patient's task is to draw a line as quickly as possible to connect the numbers in the correct order. Part B is a variation on part A with letters added, so the series looks like (1, A, 2, B, 3, C, ...). The test administrator measures the time that the patient takes to connect the numbers and letter in the correct order. The trail making test evaluates psychomotor tempo, in part A, and also set-shifting (task switching), in part B.

Stroop

During the Stroop test, a patient is presented with a list of colour names that are written in a different colour than the word refers to (e.g. word red written in blue). The patient has to name the colour in which the word is written and so inhibit the urge just to read the word itself. The test administrator measures the time that the patient takes to name all presented colours.

Phonemic verbal fluency

Phonemic verbal fluency is tested by asking the patient to say as many as possible words starting with a given letter. In this particular case, letters K, P and S were used. The final measurement is the total number of said words (K+P+S).

Test on similarities

The test on similarities measures the patient's ability to conceptualise. The patient is presented with a sequence of word pairs and asked what the words in each pair have in common (e.g. orange and banana $\rightarrow$ fruit).

Digit span

Digit span is a test that measures attention and working memory. In this test, the test administrator reads a sequence of numbers of different lengths and patient attempts to repeat them. The test is administrated in the forward (the patient repeats the numbers in the same order as they were presented) and backward (patients repeats the numbers in the reverse order of the presentation) variations. The administrator records the longest sequence the patient can repeat.

Boston naming test

Boston naming test consists of 15 line drawings of everyday objects that are arranged in increasing order of difficulty. The subject is asked to correctly name each object [19]. For each correctly named object, the patient gets one point.

Semantic verbal fluency

In this test, the patient is asked to name as many animals as possible. The test administrator recorded the total number of the named animals.

Visual object and space perception battery

The Visual object and space perception battery (VOSP) is a set of tests that measure object perception and visual space perception [20]. In this thesis, the result of the location test was used as the most representative of this battery.

In this test, the patient is presented with two squares next to each other. In one square, there are numbers at different locations and in the other square, there is a single dot. The patient is tasked to say which number's location in the first square corresponds to the dot's location in the second square. This test aims to measure the visual perception of the space.

2.2 EEG processing pipeline

For reliable estimation of the functional networks, I developed an EEG processing pipeline (Figure 2.2) that cleans the EEG data from artefacts and then estimates functional networks and their parameters. The main advantages of the proposed algorithms are that it is modular and fully automatic. The modularity ensures that particular parts of the pipeline can be easily changed or skip depending on the future requirements. The full automatisation makes it very easy to process and evaluate new patients if the study grows in the future or if there is a need to recalculate the networks with different settings.

In the processing pipeline, the EEG signals are first filtered in the frequency band of interest. After the initial filtration, the independent component analysis (ICA) is applied to decompose the signal into independent components (ICs). ICs that correspond to cardiac and ocular artefacts are identified and removed. The original EEG signals are then reconstructed from the remaining ICs. In the next step, the signals are split into 2-second epochs. For each epoch, signal parameters are computed and if they indicate an artefact, the corresponding epoch is removed. Artefact-free epochs are used to estimate functional connectivity based on the cross-spectra of the signals. The algorithm supports different connectivity measures that can be computed in multiple frequency bands. The final network is thresholded to remove weak spurious links and finally, the network parameters are calculated. In the following sections, the individual parts are described in more detail.

2.3 Signal preprocessing

2.3.1 Filtration

Filtering is an excellent tool in signal processing that is used to attenuate the artefacts that do not have an overlapping frequency spectrum with the signals of interest (e.g. muscle contractions, power line hum). Symmetric linear-phase FIR filter of order 423 (1.65 seconds) was used to bandpass filter the EEG signals between 4 and 30 Hz. The advantage of the linear-phase filter is that it introduces an equal delay at all frequencies so the signal will not change its temporal shape which is essential for the electrophysiological data [21].

2.3.2 Independent component analysis

Cardiac and ocular artefacts (CAs and OAs) unfortunately cannot be removed by simple filtering because their spectra overlap with spectra of genuine EEG signals. Independent component analysis (ICA) can be used to reliably remove those artefacts by identifying and eliminating the independent components (ICs) that correspond to CAs and OAs.

Cardiac artefacts

The ECG channel was used to identify and remove the ICs that corresponded to CAs (Figure 2.3). For this purpose, I used the MNE library [22] implementation of the cross trial phase statistics (CTPS). This method first detects the R-peaks in the ECG channel and define a 1-second window with the center defined by the R-peak. Then, the Hilbert transform is used to calculate the instantaneous phase of the ICs. Finally, the deviation of the cross trial distribution of the instantaneous phases from the uniform distribution indicates a CA and the corresponding ICs are marked for removal. The advantage of this approach is that CAs are usually decomposed into multiple ICs from which the second and third components tend to have weak peak amplitudes that may be hardly identified by its statistical properties in the amplitude domain [23]. A visual inspection of the resulting signals (Figure 2.4) confirmed a successful removal of the characteristic CA peaks while the rest of the signals remained unaltered. On average this method removed 1.94 ± 0.89 (median 2) ICs corresponding to CAs.

Ocular artefacts

The removal of OAs was inspired by Li et al. [24] who were removing OAs based on the template matching. The idea is that the ICs that correspond to OAs are easily recognisable by their distinctive scalp topographies with maxima at frontal electrodes and gradual lowering in the direction to the back of the head (Figure 2.5). In my algorithm, the IC is classified as related to an OA if the z-scores of the unmixing matrix corresponding to the Fp1, Fpz and Fp2 electrodes were higher than 3 or lower than -3. The correct functionality of the algorithm was visually inspected in several randomly chosen patients (Figure 2.6). On average this method removed 0.86 ± 0.50 (median 1) ICs corresponding to OAs.

2.3.3 Statistical thresholding

After the CA and OA artefacts were removed, the signals were split into 2-second epochs and statistical thresholding was performed to remove the epochs that still contained artefacts. The removal of the epochs that contained artefacts was inspired by an article on automated statistical thresholding by Nolan et al. [25]. The idea of the automated statistical thresholding can be described in four steps

1. Calculate signal parameters for each signal in each epoch
2. Calculate their average values over the channels
3. Calculate the z-scores over the epochs
4. Remove the epochs for which at least one of the parameters has a z-score greater than 3

For the purpose of this thesis I decided to choose the following four signal parameters

- Amplitude range
$$P_1 = \max(x) - \min(x) \tag{2.1}$$
- Variance
$$P_2 = \sigma_x^2 = \mathrm{E}\left[x - \mu_x\right] \tag{2.2}$$
- Number of zero crossings
$$P_3 = \text{number of times signal } x \text{ changes its sign} \tag{2.3}$$
- Kurtosis
$$P_4 = \mathrm{E}\left[\left(\frac{x - \mu_x}{\sigma_x}\right)^4\right] \tag{2.4}$$

where x is a time series, μ its mean, σ_x its standard deviation and $\mathrm{E}\left[\cdot\right]$ denotes the mean value of $\cdot$ [26].

The whole algorithm was recursively repeated until the z-scores for all the parameters in all the remaining epochs were not higher than 3. In this way, on average, 22 ± 11 (median 19) epochs were removed which resulted in 275 ± 11 (median 278) artefact-free epochs per patient that were used for connectivity estimation.

2.4 Spectral connectivity

2.4.1 Frequency bands

The spectral connectivity between each pair of the channels was calculated in three different frequency bands

- 4-8 Hz (theta)
- 8-13 Hz (alpha)
- 13-30 Hz (beta)

2.4.2 Connectivity measures

Let F_x and F_y be Fourier spectra of signals x and y, respectively. Cross-spectrum S_{xy} of signals x and y is defined as

$$S_{xy} = F_x F_y^* \tag{2.5}$$

where F_y^* is the complex conjugate of F_y [27]. In this thesis I use three connectivity measures based on cross-spectra, coherence, imaginary coherence and weighted phase lag index.

Coherence is a classical measurement of the linear relationship between the signals and is defined as

$$C = \frac{|\mathrm{E}\left[S_{xy}\right]|}{\sqrt{\mathrm{E}\left[S_{xx}\right]\mathrm{E}\left[S_{yy}\right]}} \tag{2.6}$$

where $\mathrm{E}[\cdot]$ denotes the mean value over the epochs. Even though the coherence is easy to calculate and interpret it is also prone to creating false connections caused by the volume conduction which is a common problem in scalp EEG. Therefore, many studies prefer to use other measures, such as imaginary coherence and weighted phase lag index that are more robust to volume conduction.

Imaginary coherence is defined as

$$ImC = \frac{\mathrm{Im}\left(\mathrm{E}\left[S_{xy}\right]\right)}{\sqrt{\mathrm{E}\left[S_{xx}\right]\mathrm{E}\left[S_{yy}\right]}} \tag{2.7}$$

This measure takes advantage of the fact that the volume conduction does not affect the imaginary part of the cross-spectrum. However, Vinck et al. [27] pointed out some shortcomings of this measure. First, the imaginary coherence still contains the real part of the cross-spectrum in its denominator and, second, the phase can strongly influence this measure because it is the most sensitive at the quarter of the cycle ($\pi/2$) at which the magnitude of the imaginary part is the highest. To overcome those problems, they defined the weighted phase lag index as

$$WPLI = \frac{|\mathrm{E}[\mathrm{Im}(S_{xy})]|}{\mathrm{E}[|\mathrm{Im}(S_{xy})|]} \tag{2.8}$$

which is thought to be superior to the imaginary coherence regarding the robustness to volume conduction [27]. The MNE library [22] implementation of those three connectivity measures was used to estimate the connectivity of the EEG recordings in this thesis.

2.5 Network thresholding

The connectivity estimators described in the previous section gives a non-zero number for each pair of the EEG channels. Network thresholding is a process,

during which the weaker links are set to 0 (i.e. removed) and the stronger connections are set to 1 (binarization). This approach aims to eliminate weak links that are caused by noise rather than by genuine EEG activity.

In my thesis, I use a proportional threshold that keeps a certain percentage of the strongest links. Unfortunately, the literature is not consistent regarding which threshold is the most appropriate. For this reason, use a range of thresholds from 20 to 80 % with a step of 1 %. The network parameters are calculated for each threshold separately and then the final values are averaged over all the (Figure 2.7).

Another problem is that the resulting graphs can become disconnected for smaller thresholds, which can affect the network measures. For this reason, I first calculate the maximum spanning tree of the graph and then I add further connections from strongest to weakest until the proportional threshold is reached.

2.6 Network parameters

In this section, I present definitions of the used network parameters and evaluate relationships among them. The source of the formulas (unless stated otherwise) is Rubinov and Sporns [2]. Table 2.2 depicts a list of all the calculated parameters and their division into domains.

2.6.1 Basic concepts

Let G be a binary (unweighted) graph representing a brain network, N is the set of all its nodes, and M is the set of all its links. The graph G has n nodes that are connected by m links. A connection (link) a_{ij} between nodes i and j is described as

$$a_{ij} = \begin{cases} 1 & \text{if link } (i, j) \text{ exists} \\ 0 & \text{otherwise} \end{cases} \tag{2.9}$$

Degree of a node i is the number of its neigbours, that is the number of nodes that have a direct link to the node i

$$k_i = \sum_{j \in N} a_{ij} \tag{2.10}$$

Let g_{ij} be the shortest path between nodes i and j. The shortest distance between nodes i and j is the number of links in g_{ij}

$$d_{ij} = \sum_{a_{uv} \in g_{ij}} a_{uv} \tag{2.11}$$

For the measures of local efficiency, it is also convenient to define the number of triangles around a node i

$$t_i = \frac{1}{2} \sum_{j,h \in N} a_{ij} a_{ih} a_{jh} \tag{2.12}$$

Time	Event
00:00	start of the examination
02:00	open eyes
02:10	close eyes
03:00	open eyes
03:05	close eyes
04:00	open eyes
04:10	close eyes
05:00	start of the hyperventilation through the nose
07:00	end of the hyperventilation through the nose
07:05	start of the hyperventilation through the mouth
09:05	end of the hyperventilation through the mouth
11:00	open eyes
11:10	close eyes
16:00	open eyes
16:10	close eyes
19:00	open eyes
19:10	close eyes
20:00	end of the examination

Table 2.1: The figure shows a standardised EEG examination sequence that was recorded with each patient. Highlighted, the starts of the closed-eye segments that were used for the resting-state connectivity estimation (in total 665 seconds).

Parameter domain	Parameter
Functional integration	characteristic path length
	global efficiency
Functional segregation	clustering coefficient
	transitivity
Centrality	closeness centrality
	betweenness centrality
Resilience	variance degree
	assortativity

Table 2.2: A list of network parameters divided into network-measure domains.

2.6.2 Functional integration

Functional integration (global efficiency) describes brain's ability to rapidly combine information from distant brain regions. Functional integration is measured by two parameters, characteristic path length and global efficiency.

Characteristic path length is the average shortest path between all pairs of nodes

$$L = \frac{1}{n} \sum_{i \in N} \frac{\sum_{j \in N, j \neq i} d_{ij}}{n-1} \tag{2.13}$$

An alternative to the characteristic path length is average global efficiency which is a parameter based on the inverse shortest path length

$$E = \frac{1}{n} \sum_{i \in N} \frac{\sum_{j \in N, j \neq i} d_{ij}^{-1}}{n-1} \tag{2.14}$$

2.6.3 Functional segregation

Functional segregation (local efficiency) refers to the network's ability to locally process information in densely interconnected groups of nodes. Functional segregation is measured by two parameters, clustering coefficient and transitivity.

Clustering coefficient is the fraction of triangles around an individual node and its average value for the whole network is given by

$$C = \frac{1}{n} \sum_{i \in N} C_i = \frac{1}{n} \sum_{i \in N} \frac{2t_i}{k_i(k_i - 1)} \tag{2.15}$$

An alternative measurement of functional segregation is transitivity that indicates the portion of existing triangles in the network

$$T = \frac{\sum_{i \in N} 2t_i}{\sum_{i \in N} k_i(k_i - 1)} \tag{2.16}$$

2.6.4 Centrality

Centrality measures the importance of the nodes in the network and is mainly used to identify hubs. There are many different measures of centrality from which I chose the closeness and betweenness centralities because they are relatively common in the literature and easy to interpret.

Closeness centrality of node i is the inverse of the average shortest path length from node i to all other nodes in the network. Its average value for the whole network is

$$CC = \frac{1}{n} \sum_{i \in N} CC_i = \frac{1}{n} \sum_{i \in N} \frac{n-1}{\sum_{j \in N, j \neq i} d_{ij}} \tag{2.17}$$

Betweenness centrality of node i is the fraction of all shortest paths in the network that pass through node i. The average betweenness centrality of the

whole network is defined as

$$BC = \frac{1}{n}\sum_{i\in N} BC_i = \frac{1}{n}\sum_{i\in N}\frac{1}{(n-1)(n-2)}\sum_{\substack{h,j\in N\\ i\neq j, i\neq h, j\neq h}}\frac{\rho_{hj}(i)}{\rho_{hj}} \tag{2.18}$$

where ρ_{hj} is the number of shortest paths between h and j, and $\rho_{hj}(i)$ is the number of shortest paths between h and j that pass through i.

2.6.5 Resilience

Network resilience refers to the brain's ability to withstand a focal insult or degenerative changes such as in Alzheimer's disease. In this thesis, I measure network resilience by variance degree and assortativity.

Variance degree [17] measures the wideness of the degree distribution and is defined as

$$VD = \frac{1}{n-1}\sum_{i\in N}(k_i - \overline{k})^2 \tag{2.19}$$

where $\overline{k}$ is an average degree.

Assortativity is a correlation coefficient between the degrees of the nodes on the opposite ends of the links

$$R = \frac{m^{-1}\sum_{(i,j)\in M} k_i k_j - \left[m^{-1}\sum_{(i,j)\in M}\frac{1}{2}(k_i + k_j)\right]^2}{m^{-1}\sum_{(i,j)\in M}\frac{1}{2}\left(k_i^2 + k_j^2\right) - \left[m^{-1}\sum_{(i,j)\in M}\frac{1}{2}(k_i + k_j)\right]^2} \tag{2.20}$$

High assortativity indicates a presence of strongly interconnected groups of high-degree nodes (hubs, rich clubs) that ensure better robustness of the network.

2.6.6 Parameter selection

A closer examination of the correlation matrix of the network parameters (Figures 2.8, 2.9) showed that those are strongly intercorrelated. For this reason, I chose the following three parameters to represent the overall quantity of the functional networks.

1. Clustering coefficient
2. Betweenness centrality
3. Variance degree

In this selection, clustering coefficient represents functional segregation and it is also highly positively correlated with assortativity.

Betweenness centrality is mainly a measure of centrality but it also has a strong negative correlation with path length and strong positive correlation with global efficiency. Therefore, the betweenness centrality also very well reflects the functional integration of the network.

Variance degree is rather uncorrelated to all other parameters.

2.7 Cognitive parameters

The administration of the neuropsychological tests (section 2.1.3) resulted in 15 relevant values for each patient and so it was desirable to reduce their dimension. To achieve this, the neuropsychologist who administrated the tests proposed six umbrella cognitive parameters. Additionally, one more parameter was derived based on the principal component analysis (PCA).

2.7.1 Derived by neuropsychologist

A skilled neuropsychologist divided the neuropsychological test into six cognitive domains (Table 2.3). The tests belonging to a particular domain were combined into a one-number parameter by calculating a mean of their z-scores. The proposed domains were

1. Global cognitive performance
2. Memory
3. Executive functions
4. Attention, working memory and psychomotor tempo
5. Speech
6. Visuospatial functions

2.7.2 Derived by PCA

Additionally, to the six cognitive parameters proposed by the neuropsychologist, a seventh parameter, global efficiency, was added. This parameter was inspired by Hawellek el al. [28] who calculated the global efficiency as the first principal component of the neuropsychological tests. In my case, the PCA of the neuropsychological tests showed, that the first principal component explained about 42 % of the total variance (Figure 2.11). This component also strongly correlated with the cognitive parameters derived by the neuropsychologist (Figure 2.10), suggesting it might be a reasonable estimation of the global cognition. The tests that mostly contributed to the first principal component were mainly related to the executive functions and verbal fluency (Figure 2.12). Those properties correspond to the observations made in the original paper by Hawellek el al. [28].

2.8 Statistical evaluation

Kendall's τ was used to estimate possible correlations between the network and cognitive parameters. The advantage of the Kendall's τ is that it is a non-parametric test and thus is robust to outliers and can also detect nonlinear

monotonic relationships. Furthermore, Kendall's τ is more appropriate for discrete data, which might be the case with some of the neuropsychological tests. It is also easy to calculate and interpret [29]. In this thesis, τ-values and their p-values were computed using a corresponding function from the SciPy library [30]. The p-value was calculated for the null hypothesis $\tau = 0$, meaning no monotonic relationship.

The correlation coefficient and its p-value were calculated multiple times to evaluate various possible relationships between the network and cognitive parameters. This repeated testing might lead to many falsely rejected true null hypothesis (some p values are small just by chance). For this reason, there are two methods used in this thesis to minimalise the reporting of falsely significant values and enhance the final interpretations. Firstly, the Benjamini-Hochberg procedure was used to adjust the significance level of the p-values. Secondly, the shapes of the resulting p-value histograms were studied. Those histograms are roughly uniform if the null hypothesis is true for every test. However, if there is a greater portion of hypothesis tests for which the null hypothesis is false, those tests will produce very small p-values (<0.05) and will cause the final histogram to be right-skewed (Figure 2.13) [31].

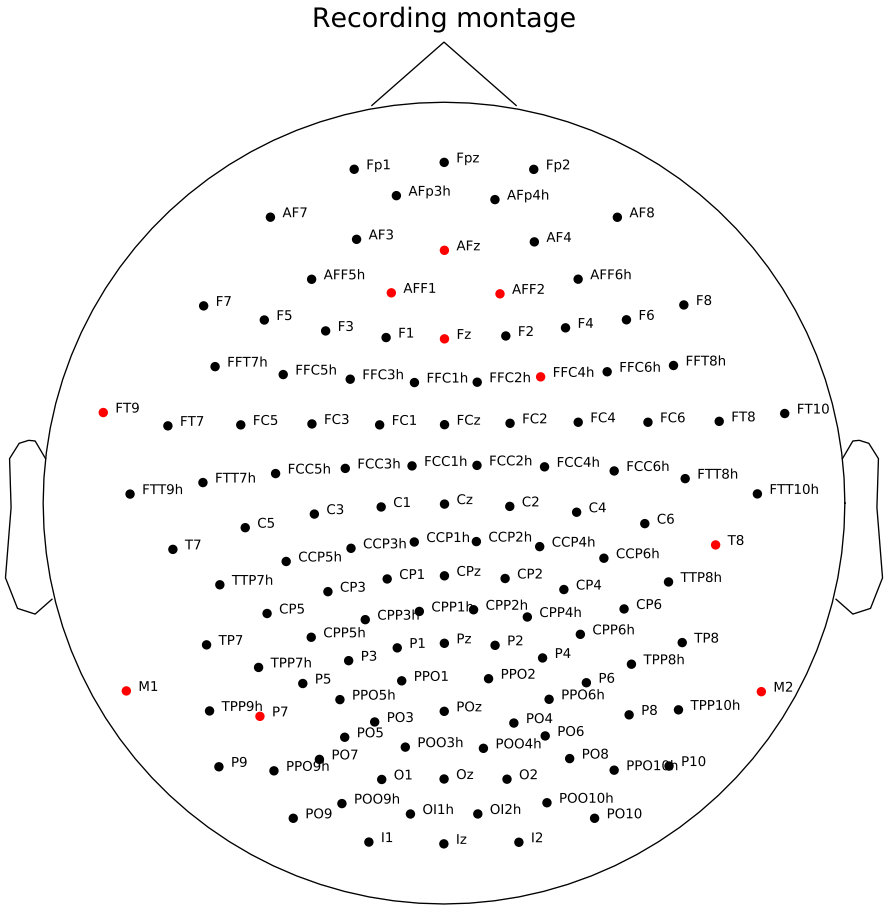

Figure 2.1: The EEG recording montage consisted of 128 electrodes. 10 of those electrodes, showed in red (AFz, AFF1, AFF2, Fz, FFC4h, FT9, T8, P7, M1, M2), were removed from the final network analysis because their signals were missing (flat, disconnected) in some of the recordings.

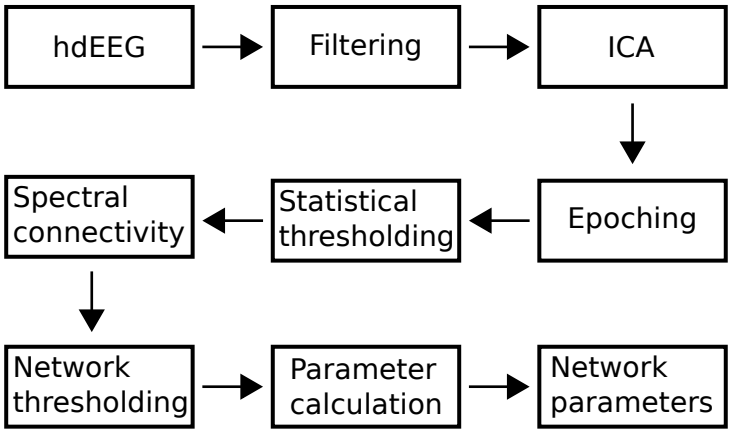

Figure 2.2: The figure shows a diagram of the EEG processing pipeline. The EEG signals are first filtered in the required frequency band. Then, independent component analysis (ICA) is used to identify and remove cardiac and ocular artefacts. Afterwards, the signals are split into 2-second epochs and statistical thresholding is performed to remove the epochs that contain artefacts. Artefact-free epochs are used to estimate functional connectivity based on the cross-spectra of the signals. The final network is thresholded to remove weak spurious links. Finally, the network parameters are calculated.

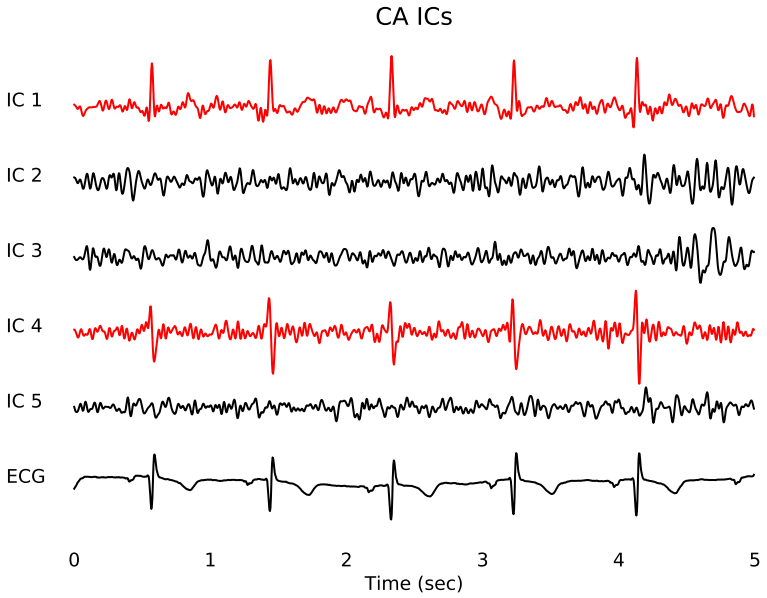

Figure 2.3: The figure shows a 5-second window illustrating five independent components (ICs) and an ECG channel for comparison. IC 1 and IC 4 (in red) correspond to cardiac artefacts (CAs). Notice their similarity to the ECG channel.

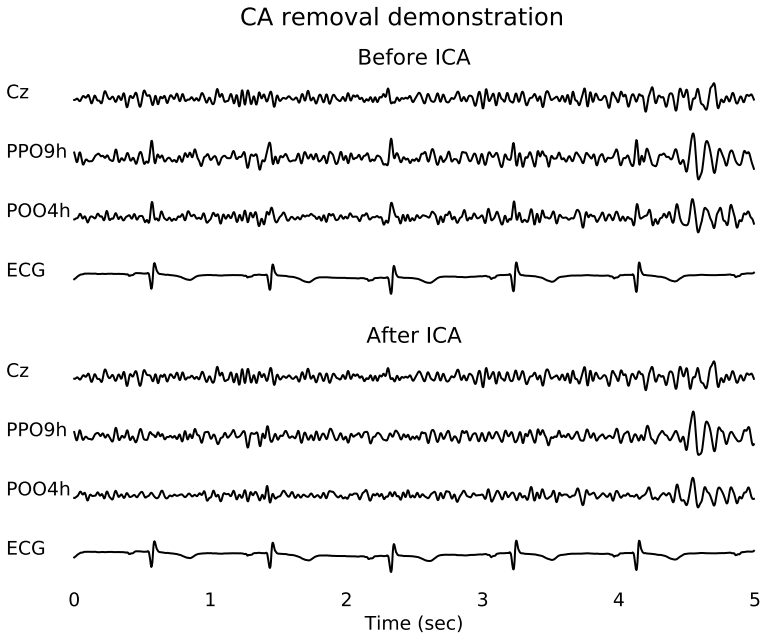

Figure 2.4: A visual inspection of the cardiac artefact (CA) removal on the example of 3 EEG channels. An ECG channel included for comparison. Notice the R-peaks leaking appearing in PPO9h and POO4h channels in the upper panel. After the artefact removal, the lower panel, those peaks disappear. The genuine EEG signal remains unaltered.

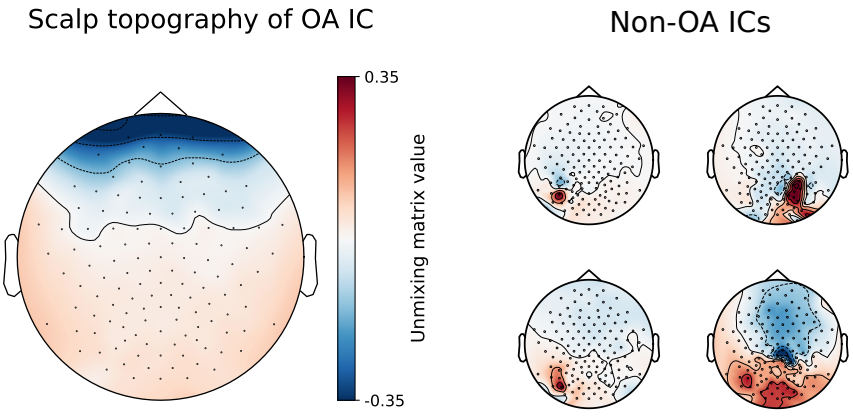

Figure 2.5: On the left-side, an example of a scalp topography of an independent component (IC) that corresponds to an ocular artefact (OA). On the right-side, for comparison, four ICs that do not represent an OA.

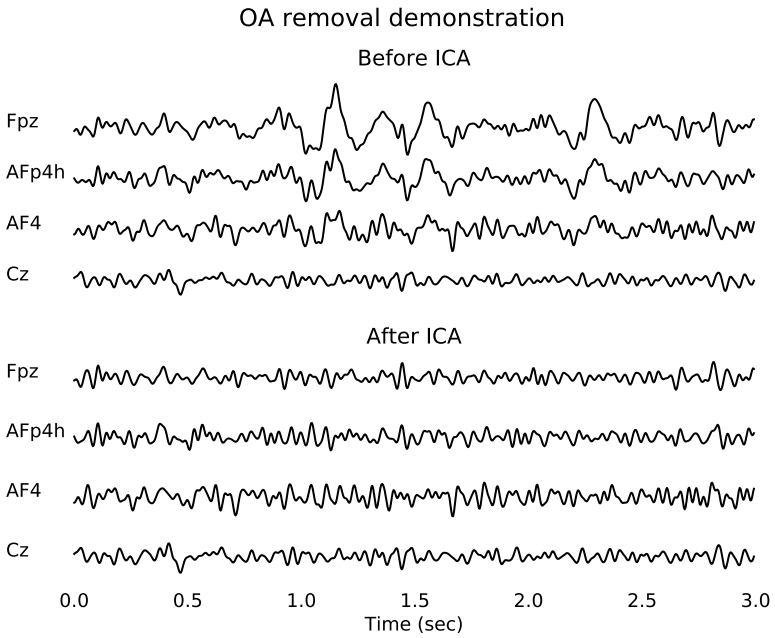

Figure 2.6: The figure shows an example of the ocular artefact (OA) removal. The upper panel shows four EEG before the ICA and the lower panel shows the same signals after the removal of OA ICs. Notice that channel Cz that does not contain any artefacts remains unaltered.

Cognitive domain	**Measure**
Global cognitive performance	Mini-mental state examination
Memory	Free recall
	Total recall
	Delayed free recall
	Delayed total recall
Executive functions	Trail making test, part B
	Phonemic verbal fluency
	Similarities
	Stroop
Attention, working memory and psycho-motor tempo	Trail making test, part A
	Digit span, forward
	Digit span, backward
Speech functions	Boston naming test
	Semantic verbal fluency
Visuospatial functions	Visual object and space perception battery

Table 2.3: A list of neuropsychological tests divided into cognitive domains. The division was proposed by the test administrator.

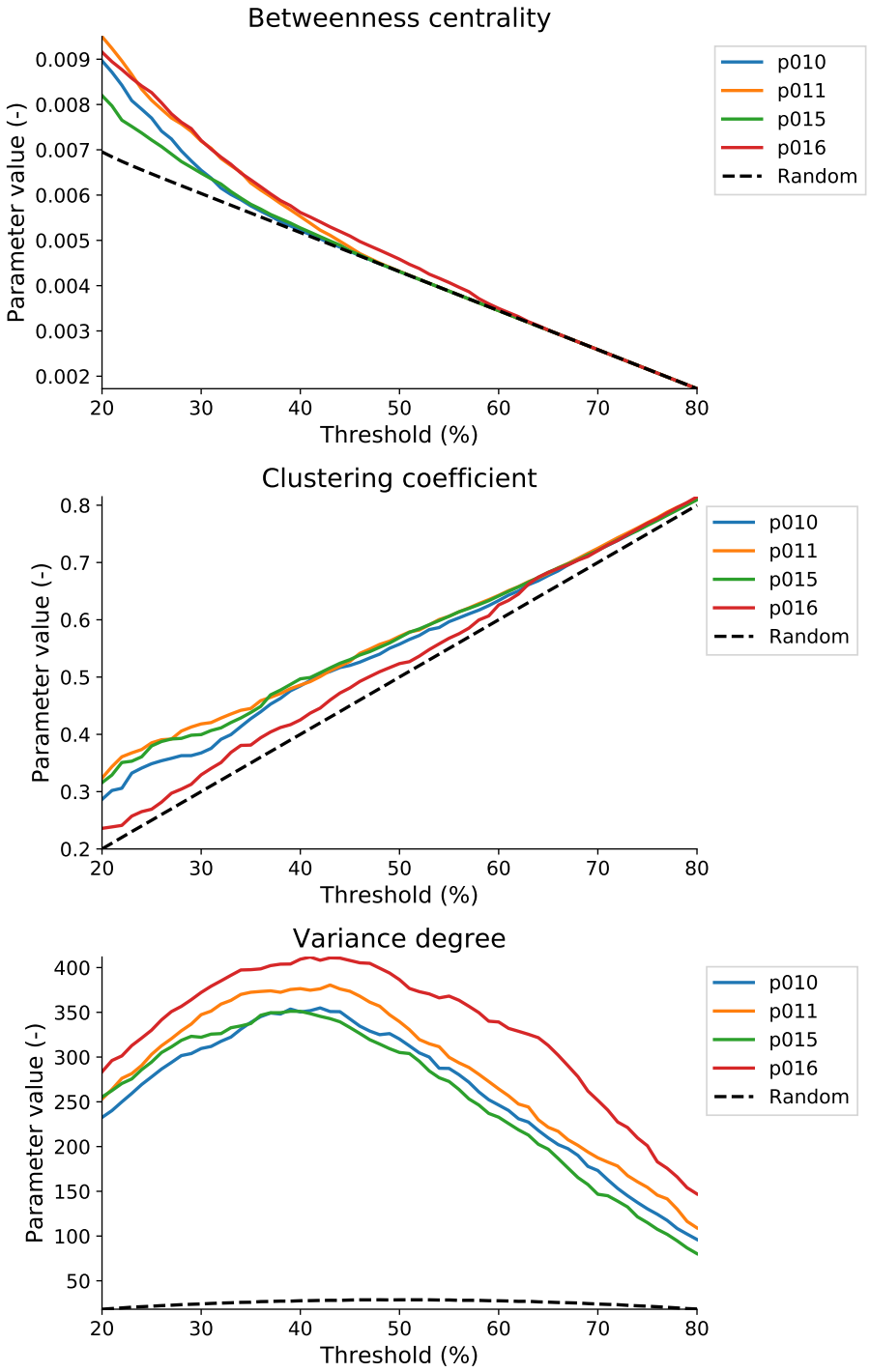

Figure 2.7: The figure shows the dependency of the parameter value on the threshold for three network parameters, betweenness centrality, clustering coefficient and variance degree. The data is shown for four randomly chosen subjects (colour lines). The dashed line shows the parameter value for a random network that was estimated based on 1000 iterations. The final network parameter for each subject is the mean over all the thresholds.

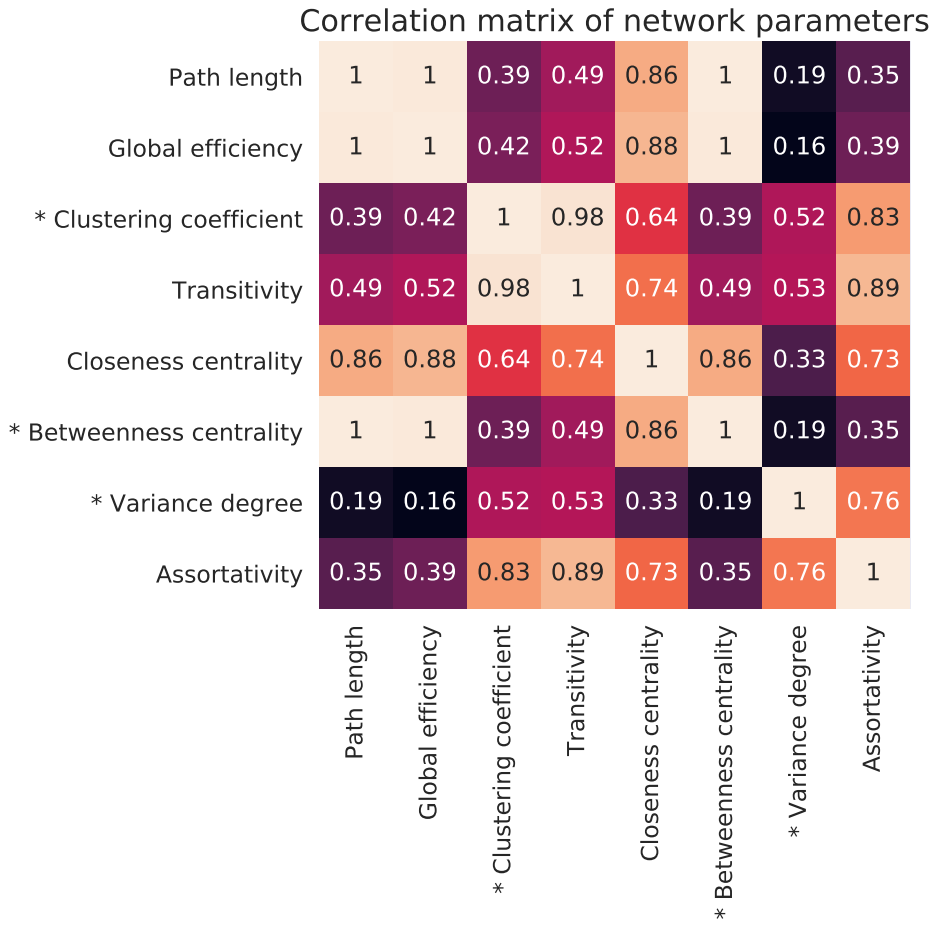

Figure 2.8: Network parameters are strongly intercorrelated. Parameters marked with a star were selected for further analysis as the representatives of the overall connectivity. The presented numbers are absolute values of the Pearson correlation coefficient. The absolute values are presented to quickly spot the strong correlations, for the original values see Figure 2.9

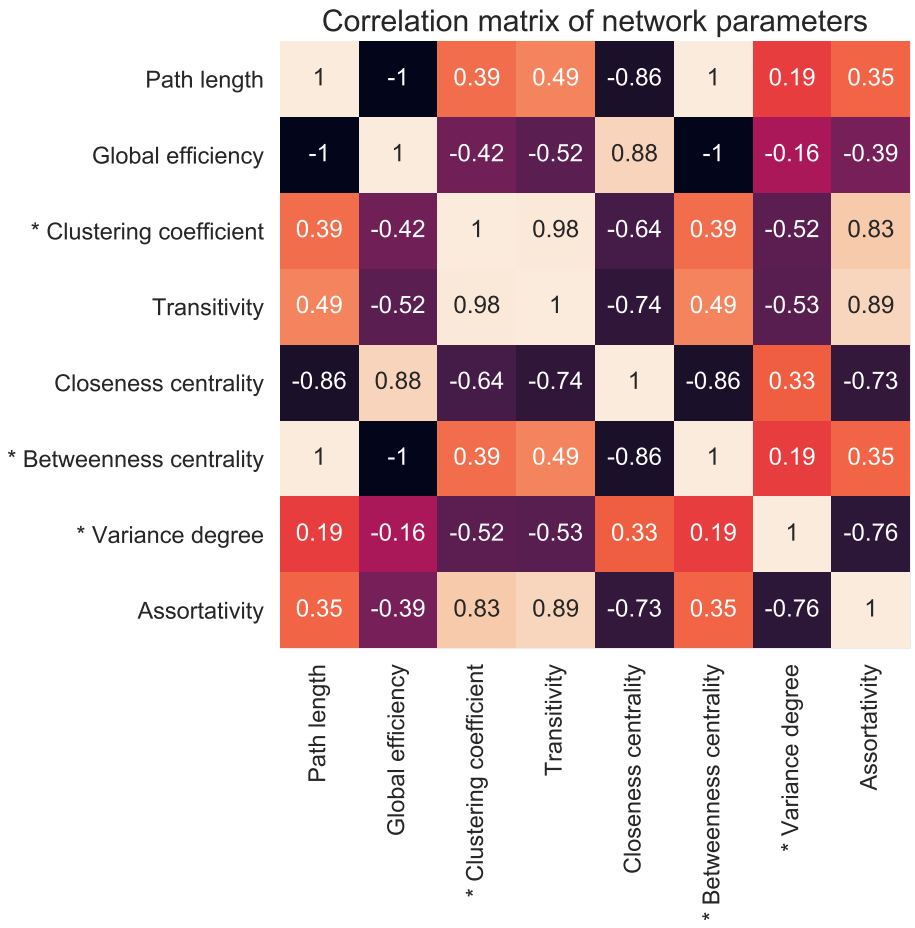

Figure 2.9: The values of the Pearson correlation coefficient for each pair-wise combination of the network parameters. The figure is the same as Figure 2.8 but it shows also the minus signs to make the interpretation of the relationships clearer.

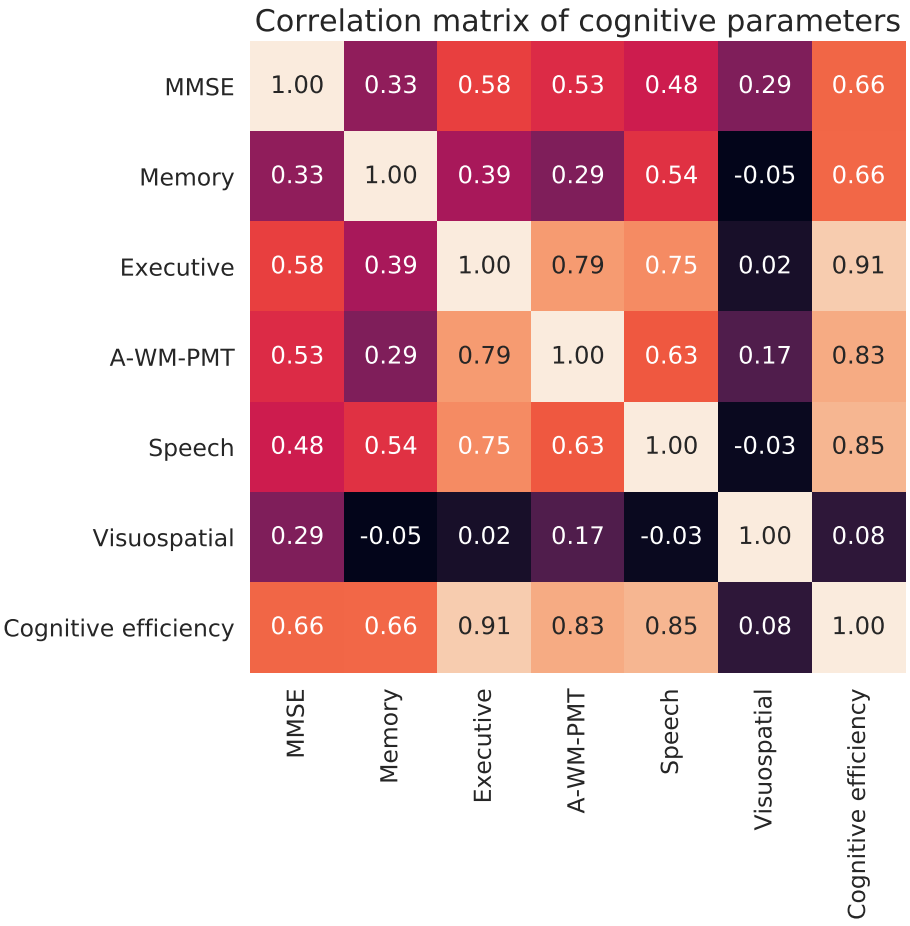

Figure 2.10: Correlation matrix of the cognitive parameters. Notice that the cognitive efficiency, a parameter derived by the PCA, is strongly and positively correlated with all the other parameters. MMSE stands for Mini-mental state examination (global cognitive performance) and A-WM-PMT stands for attention, working memory and psychomotor temp.

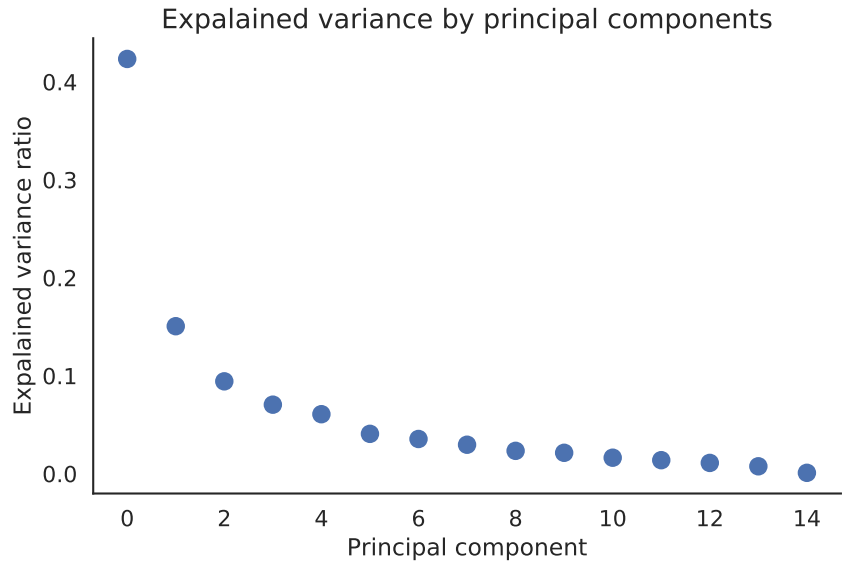

Figure 2.11: The first principal component explains over 42 % of the total variance.

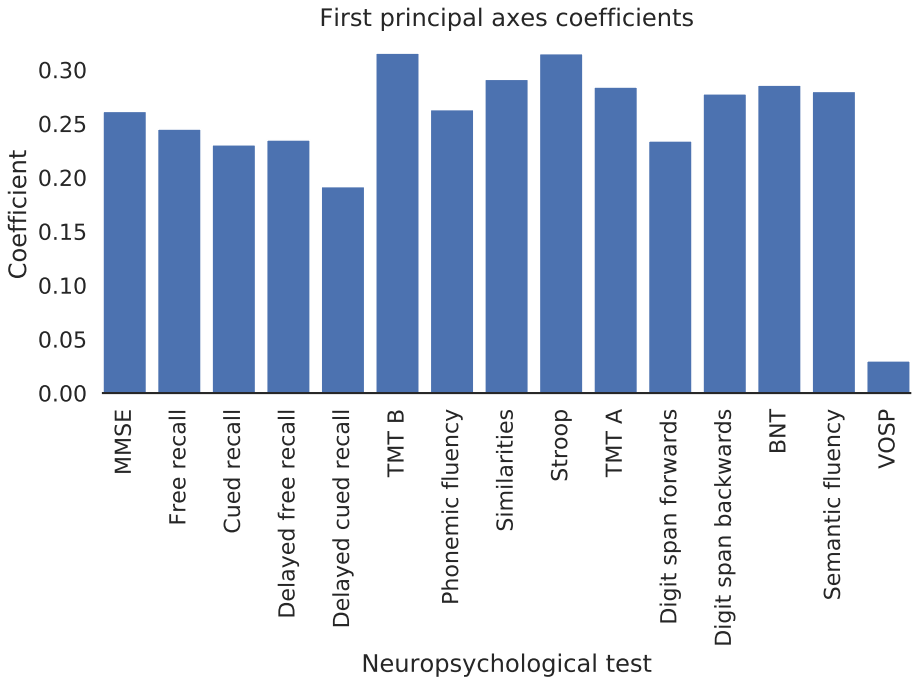

Figure 2.12: The first principal axis coefficients. The main contributors are trail making tests (TMT A, TMT B), Stroop test and the test on similarities, which mostly correspond to the executive functions.

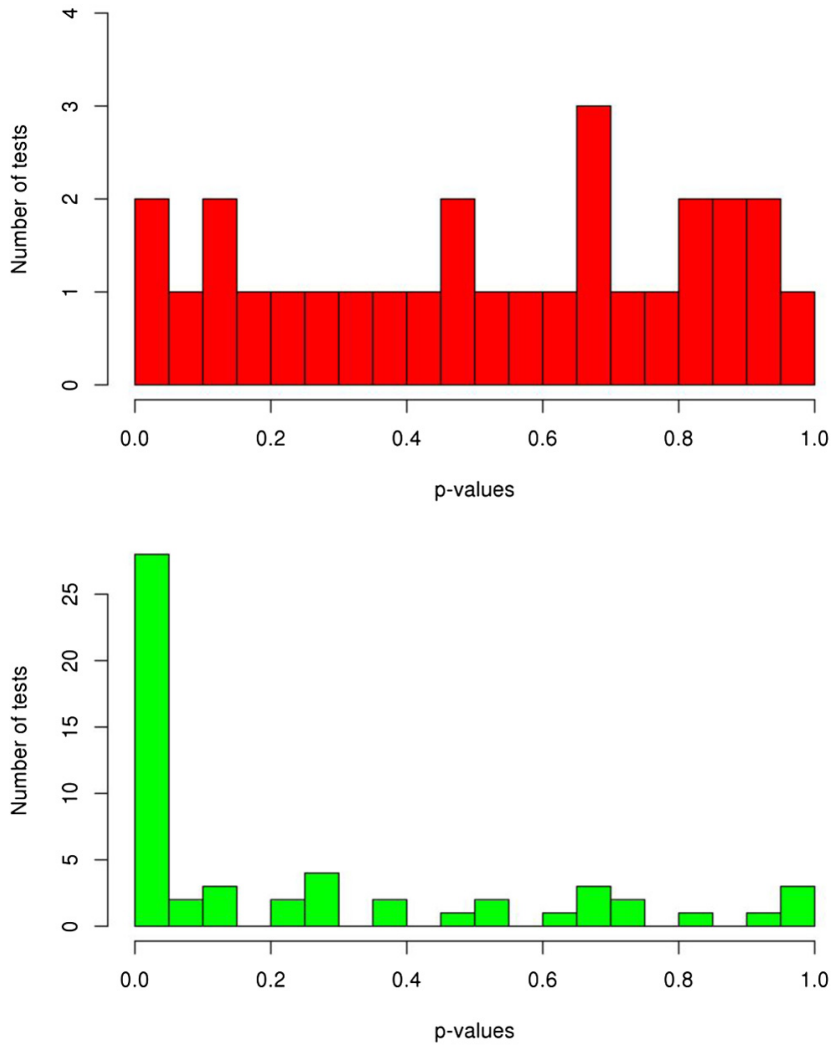

Figure 2.13: The figure illustrates histograms of p-values from two different studies. Upper histogram depicts the distribution of p-values that are roughly uniform, which indicates that the null hypothesis was true for every test. In the lower plot, small p-values are much more probable which suggests that many of the small p-values correctly rejected false null hypotheses and were not caused just by a random fluctuation (source: Glickman et al. [31]).

Chapter 3

Results

The analysis was performed on a sample of 45 post-stroke patients. For each patient, three network parameters (clustering coefficient, betweenness centrality, variance degree) were estimated by three connectivity estimators (weighted phase lag index, imaginary coherence, coherence) in three frequency bands (theta, alpha, beta) which added up to 27 parameters in total. Those parameters were compared against 7 cognitive parameters, 6 proposed by the neuropsychologist and 1 estimated by the PCA.

3.1 Overall correlations

Kendall's τ and its p-value were calculated for each network-cognitive parameter pair to test the null hypothesis that there is no relationship between the parameters. In total, 189 null hypothesis were tested from which 19 (10 %) were significantly rejected on the significance level of 0.05. However, none of the tests was significant after the Benjamini-Hochberg false discovery rate correction (Table 3.1). Figure 3.1 shows a histogram of the produced p-values that seems to be somehow right-skewed.

Out of the 19 significant tests 2 included global cognitive parameter; 1 memory; 3 executive functions; 4 attention, working memory and psychomotor tempo; 3 speech; 0 visuospatial functions; and 6 cognitive efficiency. That made the cognitive efficiency the most correlated cognitive parameter.

Regarding the significant tests and network parameters, 6 included clustering coefficient, 7 betweenness centrality, and 6 variance degree.

3.2 Connectivity estimators

The highest average Kendall's τs were observed for imaginary coherence in theta and beta frequency bands (Figure 3.2). The same result was indicated also by the ratio of significant p-values (Figure 3.3) that were 0.24 and 0.33 for imaginary coherence in theta and beta bands respectively.

In Figure 3.4, histograms of p-values for all the connectivity estimators are shown. Histograms for weighted phase lag index and imaginary coherence in theta and beta bands indicate a strong righ-skewness.

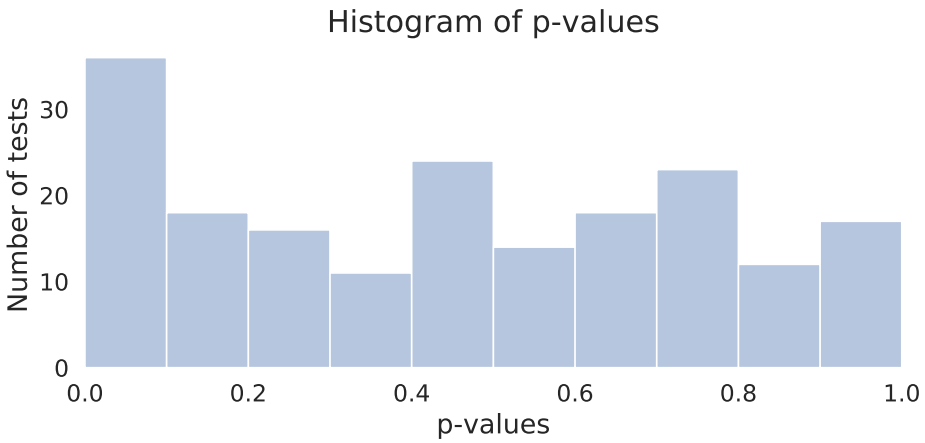

Figure 3.1: Histogram of all 189 p-values. The values are noticebly right-skewed suggesting there might be a relationship between the network and cognitive parameters.

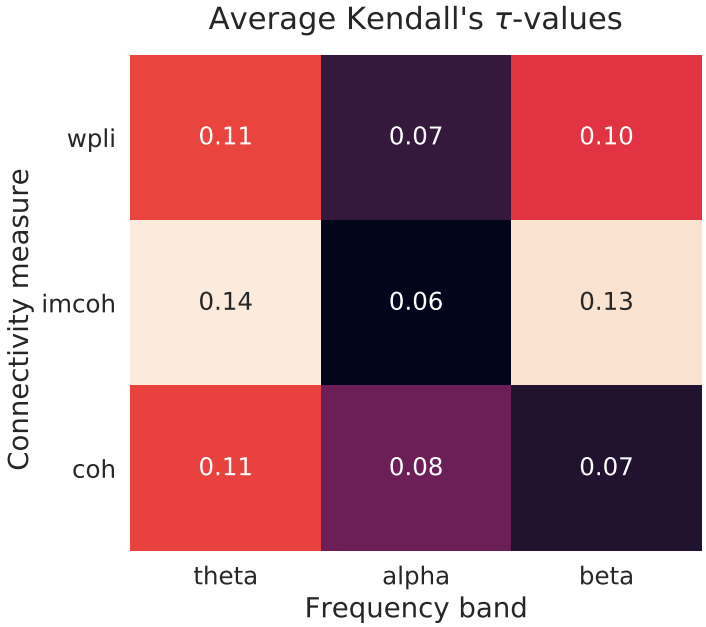

Figure 3.2: Average τ-value for each connectivity estimator, weighted phase lag index (wpli), imaginary coherence (imcoh), and coherence (coh).

Band	Cognitive parameter	Network parameter	τ	p	p*
theta	a-wm-pmt	clustering coefficient	0.29	0.005	0.34
	speech	clustering coefficient	0.21	0.041	0.45
	cognitive efficiency	clustering coefficient	0.23	0.027	0.45
beta	memory	betweenness centrality	0.21	0.043	0.45
	cognitive efficiency	variance degree	0.22	0.035	0.45

(a) : Weighted phase lag index

Band	Cognitive parameter	Network parameter	τ	p	p*
theta	executive functions	betweenness centrality	-0.22	0.030	0.45
	a-wm-pmt	clustering coefficient	0.29	0.005	0.34
	a-wm-pmt	betweenness centrality	-0.21	0.040	0.45
	cognitive efficiency	clustering coefficient	0.22	0.035	0.45
	cognitive efficiency	betweenness centrality	-0.23	0.028	0.45
beta	executive functions	betweenness centrality	0.20	0.048	0.46
	executive functions	variance degree	0.27	0.008	0.39
	a-wm-pm	variance degree	0.25	0.016	0.45
	speech	betweenness centrality	0.21	0.043	0.45
	speech	variance degree	0.21	0.043	0.45
	cognitive efficiency	betweenness centrality	0.22	0.035	0.45
	cognitive efficiency	variance degree	0.29	0.005	0.34

(b) : Imaginary coherence

Band	Cognitive parameter	Network parameter	τ	p	p*
theta	global cognition	clustering coefficient	-0.25	0.025	0.45
	global cognition	variance degree	-0.26	0.017	0.45

(c) : Coherence

Table 3.1: List of cognitive-network parameter pairs that were significantly correlated on the significance level of 0.05. The tables show the results separately for the weighted phase lag index **(a)**, imaginary coherence **(b)** and coherence **(c)**. The **p*** column depicts the p-value after the Benjamini-Hochberg correction.

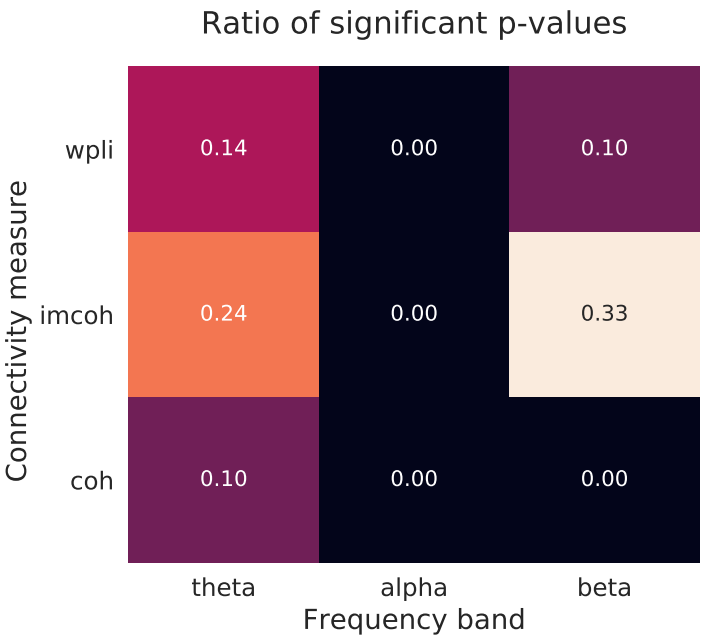

Figure 3.3: Ratio of significant p-values for each connectivity estimator, weighted phase lag index (wpli), imaginary coherence (imcoh), and coherence (coh).

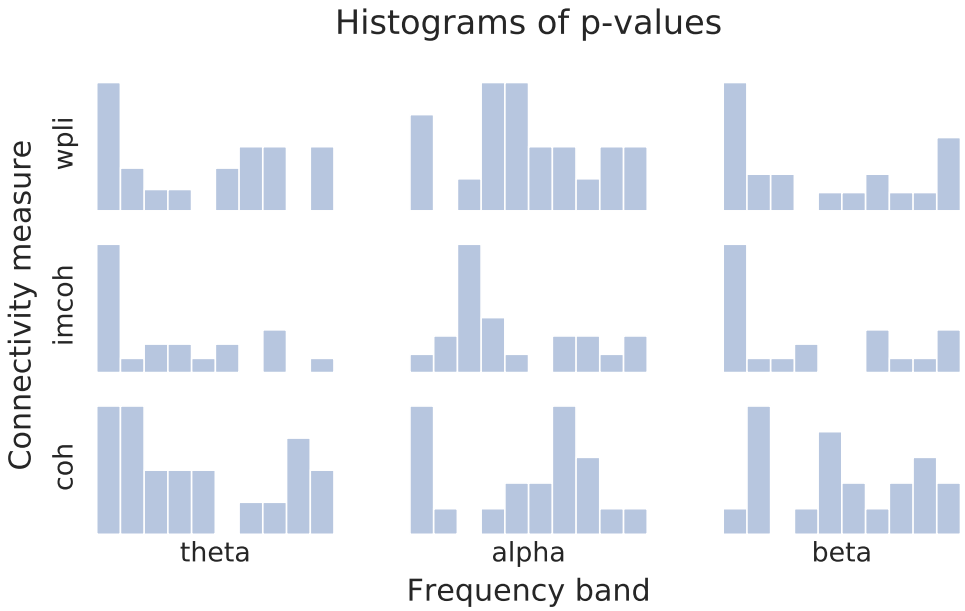

Figure 3.4: Histogram of p-values for all connectivity estimators. Notice that the histograms for the weighted phase lag index and imaginary coherence in the theta and beta bands are strongly right-skewed. wpli indicates weighted phase lag index, imcoh imaginary coherence, and coh coherence.

Chapter 4

Discussion

In this thesis, I correlated cognitive and network parameters of 45 post-stroke patients. None of the tested relationships showed a significant relationship after the Benjamini-Hochberg correction. However, the resulting histogram of p-values (Figure 3.1) was considerably right-skewed, implying there might be some correctly rejected null hypotheses worth further exploring.

I explored the data more closely by plotting the p-value histograms separately for each pairwise combination of a connectivity measure and a frequency band (Figure 3.4). The resulting histograms showed very high right-skewness for the weighted phase lag index (WPLI) and imaginary coherence in theta and beta bands. Furthermore, for the imaginary coherence in theta and beta bands, the percentage of p-values smaller than 0.05 reached 24 and 33 % respectively, which is far more that one would expect by pure chance. The better results for the WPLI and imaginary coherence as in comparison with coherence are interesting because those two measures are less affected by the volume conduction which might be the reason why the standard coherence showed less significant correlations.

There were no significant results in the alpha band. Findings in the beta band are saying that the betweenness centrality and variance degree is getting bigger along with the bigger cognitive performance. Interestingly, in the theta band, the higher cognitive performance is reflected by lower betweenness centrality and higher clustering coefficient. Those differences between the changes in the beta and theta bands might suggest different nature of the reorganisation in distinct frequency bands.

Interestingly, in some previous studies [14, 15, 17], the authors also observed changes in the beta band connectivity related to cognitive decline. However, it is a little bit tricky to compare the exact results with those studies because of the different methodology used in each of them. Nevertheless, it is clear that the quality of the connectivity in the beta band changes in correlation with the cognitive decline.

A lot of effort in this thesis was dedicated to the development of the whole protocol that leads from the raw EEG and neuropsychological data to the final statistical comparison of the network and cognitive parameters. The independent component analysis reliably removes cardiac and ocular artefacts and the averaging of the network parameters over multiple thresholds adds

to the final robustness of the network parameters.

In collaboration with a neuropsychologist, we derived a set of cognitive parameters from the neuropsychological tests. The most correlated cognitive parameter was global efficiency, which is the parameter that was calculated based on the PCA as compared to the parameters that were proposed by the neuropsychologist. Therefore, this parameter could present a favourable one-number representation of the entire battery of the neuropsychological tests.

In some studies, the authors, instead of the raw neuropsychological tests, use their deviations from the age and education norms. That is because many of the administrated tests are strongly influenced by age, education and also sex, which might distort the measured values. Nevertheless, the network parameters were also shown to be influenced by age and sex.

Volume conduction is a common problem of the EEG recordings. In this thesis, the network parameters that were calculated based on the functional connectivity measures less sensitive to volume conduction (WPLI, imaginary coherence) showed stronger correlations with cognitive parameters than the network parameters estimated from the coherence networks. As stated in the literature [9], also in my case, coherence led to lattice-like networks similar to Figure 1.6. In those networks were observable two main clusters in frontal and occipital areas, possibly due to strong alpha activity. The WPLI and imaginary coherence networks contained more connections across the whole brain connecting nodes representing different anatomical structures. Even though the WPLI and imaginary coherence are robust to volume conduction, it is a question whether they do not ignore connections between neighbouring regions that actually should be connected. We should also ponder whether the presented EEG functional networks represent actual brain networks or are just a quantitative description of the changes in the observable EEG activity. For example, source reconstruction techniques might be applied to work with the time series that are related to the actual neural sources rather than scalp electrodes.

Chapter 5

Conclusion

In this thesis, I developed an automatic algorithm for the estimation of the network parameters from the EEG recordings. The algorithm is very variable and offers evaluation of several network parameters based on various connectivity measures and frequency bands. In cooperation with a neuropsychologist, we also prepared a favourable parametrisation of the neuropsychological tests and converted them into cognitive parameters. Finally, the network and cognitive parameters were correlated with some significant values found mainly in the theta and beta bands. However, those correlations were rather weak, and so it is not possible to conclude that there is any significant association between the network and cognitive parameters.

Nevertheless, this thesis presented methods and ideas that can be built upon in future research on this topic. Mainly, the algorithm for the network parameter estimation is easily editable and reusable and so are the methods for the parametrisation of the neuropsychological tests. I also showed some potentially interesting correlations in theta and beta bands that can be further explored in the prospective research on this topic.

In the future, it would be interesting to repeat this study on a larger group of patients. The changes in the connectivity could also be examined from a different point of view. For example, we could study the functional connectivity and cognitive decline in a longitudinal study and consequently obtain a better insight into the dynamics of the changes that those parameters undergo after a stroke. It would also be beneficial to recruit a group of healthy controls and compare their networks to the networks of post-stroke patients.

Bibliography

[1] E. Bullmore and O. Sporns. Complex brain networks: graph theoretical analysis of structural and functional systems. *Nat. Rev. Neurosci.*, 10:186–198, 2009.

[2] M. Rubinov and O. Sporns. Complex network measures of brain connectivity: Uses and interpretations. *Neuroimage*, 52:1059–1069, 2010.

[3] C. Stam. Modern network science of neurological disorders. *Nat. Rev. Neurosci.*, 15:683–695, 2014.

[4] C. Gerloff and M. Hallett. Big news from small world networks after stroke. *Brain*, 133:952–955, 2010.

[5] E. van Straaten and C. Stam. Structure out of chaos: Functional brain network analysis with EEG, MEG, and functional MRI. *Eur. Neuropsychopharmacol.*, 23:7–18, 2013.

[6] A. Rehme and C. Grefkes. Cerebral network disorders after stroke: evidence from imaging-based connectivity analyses of active and resting brain states in humans. *J. Physiol.*, 591:17–31, 2013.

[7] A. Baldassarre, L. Ramsey, J. Siegel, G. Shulman, and M. Corbetta. Brain connectivity and neurological disorders after stroke. *Curr. Opin. Neurol.*, 29:706–713, 2016.

[8] E. Carrera and G. Tononi. Diaschisis: past, present, future. *Brain*, 137:2408–2422, 2014.

[9] L. Peraza, A. Asghar, G. Green, and D. Halliday. Volume conduction effects in brain network inference from electroencephalographic recordings using phase lag index. *J. Neurosci. Methods*, 207:189–199, 2012.

[10] M. Christodoulakis, A. Hadjipapas, E. Papathanasiou, M. Anastasiadou, S. Papacostas, and G. Mitsis. Graph-theoretic analysis of scalp EEG brain networks in epilepsy – the influence of montage and volume conduction. In *13th IEEE International Conference on BioInformatics and BioEngineering, IEEE BIBE 2013*, 2013.

[11] J. Wu, E. Quinlan, L. Dodakian, A. McKenzie, N. Kathuria, R. Zhou, R. Augsburger, J. See, V. Le, R. Srinivasan, and S. Cramer. Connectivity measures are robust biomarkers of cortical function and plasticity after stroke. *Brain*, 138:2359–2369, 2015.

[12] L. Wang, X. Guo, Z. Jin J. Sun and, and S. Tong. Cortical networks of hemianopia stroke patients: a graph theoretical analysis of EEG signals at resting state. In *Conf. Proc. IEEE Eng. Med. Biol. Soc.*, 2012.

[13] F. Fallani, F. Pichiorri, G. Morone, M. Molinari, F. Babiloni, F. Cincotti, and D. Mattia. Multiscale topological properties of functional brain networks during motor imagery after stroke. *Neuroimage*, 83:438–449, 2013.

[14] M. Klados, C. Styliadis, C. Frantzidis, E. Paraskevopoulos, and P. Bamidis. Beta-band functional connectivity is reorganized in mild cognitive impairment after combined computerized physical and cognitive training. *Front. Neurosci.*, 10:1–12, 2016.

[15] C. Stam, Y. van der Made, Y., Pijnenburg, and Ph. Scheltens. EEG synchronization in mild cognitive impairment and Alzheimer's disease. *Acta Neurol. Scand.*, 108:90–96, 2003.

[16] F. Vecchio, F. Miraglia, D. Quaranta, G. Granata, R. Romanello, C. Marra, P. Bramanti, and P. Rossini. Cortical connectivity and memory performance in cognitive decline: A study via graph theory from EEG data. *Neuroscience*, 316:143–150, 2016.

[17] E. Kinney-Lang, M. Yoong, M. Hunter, K. Tallur, J. Shetty, A. McLellanc, R. Chin, and J. Escudero. Analysis of EEG networks and their correlation with cognitive impairment in preschool children with epilepsy. *Epilepsy Behav.*, 90:45–56, 2019.

[18] V. Pangman, J. Sloan, and L. Guse. An examination of psychometric properties of the mini-mental state examination and the standardized mini-mental state examination: Implications for clinical practice. *Appl. Nurs. Res.*, 13:209–213, 2000.

[19] M. Calero, L. Arnedo, E. Navarro, M. Ruiz-Pedrosa, and C. Carnero. Usefulness of a 15-item version of the boston naming test in neuropsychological assessment of low-educational elders with dementia. *J. Gerontol. B Psychol. Sci. Soc. Sci.*, 57B:P187–P191, 2002.

[20] I. Herrera-Guzman, Pena-Casanova, J. Lara, E. Gudayol-Ferre, and P. Bohm. Influence of age, sex, and education on the visual object and space perception battery (VOSP) in a healthy normal elderly population. *Clin. Neuropsychol.*, 18:385–394, 2004.

[21] A. Widmann, E. Schroger, and Burkhard Maess. Digital filter design for electrophysiological data – a practical approach. *J. Neurosci. Methods*, 250:34–46, 2015.

[22] A. Gramfort, M. Luessi, E. Larson, D. Engemann, D. Strohmeier, C. Brodbeck, L. Parkkonen, and M. Hamalainen. MNE software for processing MEG and EEG data. *Neuroimage*, 86:446–460, 2014.

[23] J. Dammers, M. Schiek, F. Boers, C. Silex, M. Zvyagintsev, U. Pietrzyk, and K. Mathiak. Integration of amplitude and phase statistics for complete artifact removal in independent components of neuromagnetic recordings. *IEEE Trans. Biomed. Eng.*, 55:2353–2362, 2008.

[24] Y. Li, Z. Ma, W. Lu, and Y. Li. Automatic removal of the eye blink artifact from EEG using an ICA-based template matching approach. *Physiol. Meas.*, 27:425–436, 2006.

[25] H. Nolan, R. Whelan, and R. Reilly. FASTER: Fully automated statistical thresholding for EEG artifact rejection. *J. Neurosci. Methods.*, 192:152–162, 2010.

[26] D. Zwillinger and S. Kokoska. *CRC Standard Probability and Statistics Tables and Formulae*. Chapman & Hall/CRC, 2000.

[27] M. Vinck, R. Oostenveld, M. van Wingerden, F. Battaglia, and C. Pennartz. An improved index of phase-synchronization for electrophysiological data in the presence of volume-conduction, noise and sample-size bias. *Neuroimage*, 55:1548–1565, 2011.

[28] D. Hawellek, J. Hipp, C. Lewis, M. Corbetta, and A. Engela. Increased functional connectivity indicates the severity of cognitive impairment in multiple sclerosis. *Proc. Natl. Acad. Sci. U.S.A.*, 108:19066–19071, 2011.

[29] M. Schaeffer and E. Levitt. Concerning Kendall's tau, a nonparametric correlation coefficient. *Psychol. Bull.*, 53:338–346, 1956.

[30] Eric Jones, Travis Oliphant, Pearu Peterson, et al. SciPy: Open source scientific tools for Python, 2001–2019. Online at `http://www.scipy.org/`; accessed May 22, 2019.

[31] M. Glickman, S. Rao, and M. Schultz. False discovery rate control is a recommended alternative to bonferroni-type adjustments in health studies. *J. Clin. Epidemiol.*, 67:850–857, 2014.